# Role of halloysite nanotubes on mechanical properties of glass fabric reinforced epoxy hybrid composites

**Madaiah DC[1], Anand A[1*] Somashekar HM[2] and Suresha B[1*]**

[1]Department of Mechanical Engineering, The National Institute of Engineering, Mysuru-570008, India

[2]Department of Mechanical Engineering, Dr. Ambedkar Institute of Technology, Bengaluru, India

[*]Corresponding Authors: emails: anand@nie.ac.in; sureshab2004@yahoo.co.in

## ABSTRACT

This study aimed to assess the impact of halloysite nanotubes (Hnts) on the mechanical characteristics of bi-directional glass fabric reinforced LY556epoxy hybrid nanocomposites. Initially, epoxy was mixed with Hnts (0 to 8 wt %) using ultrasonication and the hybrid nanocomposites were created by hand lay-up method. In accordance with ASTM guidelines, mechanical loading was applied to the created hybrid nanocomposites in order to define their local mechanical properties. The mechanical characteristics of the hybrid nano composites, including Shore D hardness, tensile strength, tensile modulus, interlaminar shear strength, flexural strength, and flexural modulus, increased as the Hnts loading increased up to 6 wt %. Using a scanning electron microscope, the chosen tensile-broken samples were analyzed to identify the sort of failure.

**Keywords:** Hybrid nanocomposites; Hand lay-up process; Hardness, Mechanical properties; Fractography

## 1. INTRODUCTION

A family of thermosetting polymers known as epoxy resins is extensively employed in many different industries, including consumer products, sports goods, electronics, shipbuilding, transportation, and building materials [1-4]. Epoxy resins also have good strength and outstanding adhesion. Because of their superior properties, fiber and micro/nanofiller reinforced polymer composite materials are therefore widely employed in current automobiles, aircraft, bearings, sleeves, and marine structures [5-8]. The strength-to-weight ratio, excellent corrosion resistance, resistance to wear, fatigue resistance, and

flexibility to be produced under difficult geometries are the most rational justifications for their utilization [9–11]. Furthermore, the fundamental features of pristine polymers surely limit their use. In this instance, new, high-performing polymer materials are receiving a lot of attention in an effort to enhance their properties and expand their uses. As a result, they have inexpensive costs, easy processing, and good strength to weight ratios [12]. However, because of their fundamentally poor thermal, electrical, conductivity, and ductile mechanical properties, virgin polymers' applications—such as epoxy/vinyl ester matrices—are typically limited.

Pristine epoxy resin is brittle due to its decreased impact strength and elongation at break. Its stiffness and hardness, however, are enough for packaging uses. Several researchers want to incorporate reinforcing materials (fiber and functional fillers) into the epoxy matrix for load-bearing applications [9-12]. Their main function is to improve the mechanical characteristics, such as fatigue, hardness, strength, stiffness, and impact energy. On the other hand, they also aim to enhance physical attributes like electrical, mechanical, or thermal sensitivity, as well as fire resistance.

Fiber-reinforced polymer composites (F-RPCs) have the potential to significantly improve resource conservation and energy efficiency when used in lightweight constructions. When structural performance is required, glass- or carbon-reinforced thermoset epoxy composites are typically chosen over other F-RPCs. Since epoxies have superior mechanical qualities and resistance to environmental deterioration than most other resin types, they are virtually exclusively used in aviation components [2, 6-8, 11, 12]. Because of their notable elasticity modulus and ability to prevent crack propagation, several scientists have used nanoparticles such as carbon nanotubes, graphene, alumina, silicon carbide, silicon dioxide, clay, zirconium oxide, and boron nitride to highlight the mechanical characteristics of synthetic fiber reinforced epoxy composites [13-16]. More specifically, halloysite nanotubes (Hnts) has evolved to be accepted as filler for reinforcement in different polymer matrices. Otherwise, due to their highly desired multi-functionality properties, F-RPCs containing nano-fillers have drawn a lot of attention recently.

Lal and Markand [17] used several percentages of hardened resin (0.25, 0.5, 0.75, and 1 phr) to examine the impact of introducing CNTs to GF-RPCs when subjected to flexural and interlaminar shear loading. They found that the highest mechanical properties are exhibited by CNTs at 0.75 phr, which results in improvements of 15.7% and 9.2%, respectively, in flexural strength and interlaminar shear strength. Epoxy composites reinforced with basalt

fibers and modified with nano-graphene oxide were examined by Mostovoy et al. [18]. The findings demonstrate that, in comparison to the unfilled composite tensile strength of 160 MPa, the samples containing 0.5 wt % of graphene oxide had higher tensile strength of 1830 MPa. For the redesigned composite, there were improvements in the tensile modulus of 31% and 19%, but only in the flexural strength of 9% and 13%. The effects of silica-graphene oxide loading and graphene oxide modification on the mechanical properties of basalt/epoxy composite were studied by Jamali et al. [19]. The specimens' maximum mechanical strength was achieved at 0.4 wt% silica-graphene. Chang [20] investigated the effects of GF-RPCs and carbon-fiber-reinforced polymer composites with MWCNT additions. According to reports, the inclusion of MWCNTs increased the flexural strength by 22.16% and the tensile strength by 34.7%. Josh et al. [21] included filler in the form of nano-graphene oxide, epoxy as matrix, and carbon fiber as strengthening agent. With the inclusion of the nanoparticles, they observed an increase in interlaminar shear strength (ILSS) of 15% and an improvement in crosswise tensile strength of 8%.

The tribological and electrical characteristics of epoxy composites loaded with nano-silica were examined by Veena et al. [22]. The outcomes show how silica loading affects the epoxy's resistance to wear. Additionally, the results of electrical parameters including dielectric strength, arc resistance, and tracking resistance clearly show the impact of silica loading on epoxy. Tian et al. [23] improved the interfacial properties of the polymers and the fibers by using epoxy matrix consisting of sol–gel silica nanocomposites. In a related study, Zheng et al. [24] treated epoxy resin with nano-silica and then employed the modified resin as matrix system in composites reinforced with glass fibers. The tensile strength and modulus were increased under tensile loading by 24% and 22%, respectively. The compressive strength and ILSS improved near 13% and 14%, respectively, however this gain was comparatively smaller. Additionally, the strength rose by 22% during bending.

Because of its low cost, improved mechanical performance, and cylindrical structure, halloysite, an aluminosilicate clay material is common nanofiller used in various polymers [25]. In order to maintain and regulate biomolecules, medications, or bioactive materials, these are frequently employed as nanofillers and nanocontainers [26–28]. El-baky and Attia [29] investigated how various wt % of Hnts affected the mechanical characteristics of epoxy composites incorporated with glass layers ate and aluminum sheets. The outcomes showed that the composites' mechanical characteristics are maximally improved when 1 wt % of Hnts is added. The mechanical properties of epoxy/graphene and epoxy/halloysite nanocomposites

were investigated by Lubomír Lapčík et al. [30]. They observed that adding I wt % graphene to the epoxy matrix enhanced ductility. Nonetheless, it was discovered that the epoxy/Hnts nanocomposites had diminishing mechanical rigidity, as evidenced by a lower Young's modulus of elasticity.

Consequently, the mechanical characteristics of glass fiber reinforced composite materials are affected by the addition of nanoparticles in both positive and negative ways. The following factors affect a nano-level hybrid composite's change in properties: (i) filler geometry; (ii) filler type; (iii) kind of resin; (iv) filler loading; (v) distribution of nanoparticles in resin; as well as (vi) fabrication method. In order to enhance mechanical properties, the current effort attempts to optimize the Hnts loading (0 to 8 wt %). There were four distinct mechanical tests carried out: hardness, tensile, interlaminar shear, and three-point bending. The matrix material utilized in this study was epoxy matrix material, and the reinforcement was provided by bidirectional E-glass plain weave woven mats.

## 2. MATERIALS and EXPERIMENTAL METHODS

### 2.1 Materials

The modified diglycidyl ether of bisphenol A-based epoxy (LY556, medium viscosity, epoxide equivalent weight of 180-190 g/eq) was the resin matrix used in this investigation. The hardener was polyamine amide (HY951) from Huntsman, Hindustan Ciba-Geigy Ltd, India. In accordance with the manufacturer's guidelines, the epoxy- polyamine amide ratio was 100:12 by weight percentage. Glass fiber (produced by Hayael Aerospace India Private Limited in Chennai, India) was utilized primarily as reinforcement in the form of 300 $g/m^2$ plain-woven fabrics. The source of the halloysite nanotubes (Hnts) was Sigma Aldrich, Bangalore, India. The cylindrical Hnts have a length ranging from 1µm to 3 µm with an mean particle diameter of 30 nm - 70 nm. According to quotes, the density of Hnts is 2.53 $g/cm^3$. The HNTs have a surface area of 64 $g/m^2$.

### 2.2 Fabrication of hybrid nanocomposites

Hnts filled G/E composites were created using the hand lay-up method in conjunction with ultrasonication. In order to prevent the formation of aggregates linked to nanofillers, ultrasonication was introduced [31]. Vibration in this ultrasonication creates sinusoidal zones of higher and lower pressure. At low pressure, microscopic cavities are created, and at high pressure, these cavities collapse. The entire process occurs at the micro-scale, releasing

energy that breaks down the aggregates around the voids and facilitates the uniform dispersion of nanofiller.

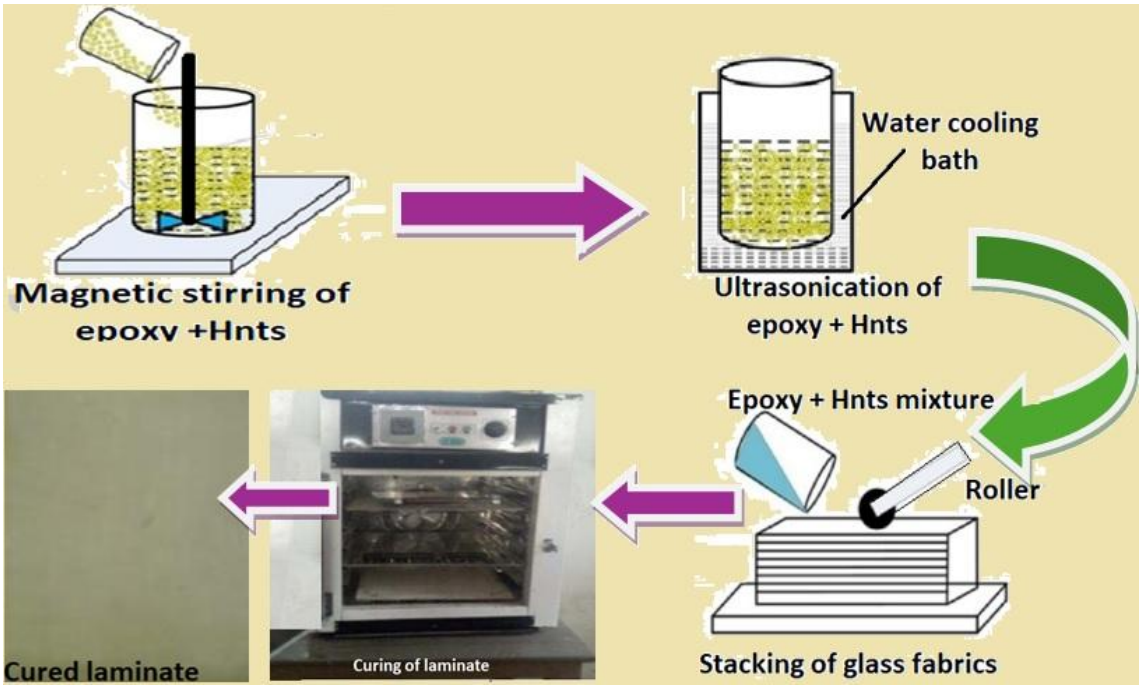


**Fig. 1** Schematic representation of the process used to fabricate nanocomposite laminates

**Table 1.** Different compositions used in hybrid nanocomposites preparation.

| Nanocomposites (Designation) | Epoxy (wt %) | Hnts (wt %) | Glass fiber (wt %) |
|---|---|---|---|
| Glass fabrics/Epoxy (H0) | 50 | 0 | 50 |
| Hnts/Glass fabrics/Epoxy (H1) | 48 | 2 | 50 |
| Hnts/Glass fabrics/Epoxy (H2) | 46 | 4 | 50 |
| Hnts/Glass fabrics/Epoxy (H3) | 44 | 6 | 50 |
| Hnts/Glass fabrics/Epoxy (H4) | 42 | 8 | 50 |

To eliminate any moisture content, the Hnts and glass mats were first positioned in an air circulated oven set at 125$^{o}$C for 3 h. The schematic representation of the process used to fabricate nanocomposite laminates is displayed in Figure 1. Table 1 lists the weight ratios of the epoxy matrix, HNTs, and glass fiber in the hybrid nanocomposites. In the current work, epoxy and Hnts mixture was subjected to a one-hour ultrasonication at 22 kHz. The beaker containing the epoxy and Hnts mixture was submerged in an ice-bath during ultrasonication to prevent epoxy deterioration from overheating.

For the fabrication of laminates, the ultrasonicated epoxy and Hnts mixture was used. Glass fiber mat was cut to the necessary size, and then a 10:1.2 combination of epoxy and Hnts was applied, along with HY951 hardener. The slurry was then applied to the glass fiber mat using a roller. Ten layers of glass fiber mat were arranged similarly. After that, it was endorsed to cure for 24 h at 0.5 MPa pressure. To post-cure, the item was placed in an oven set to 100°C for one hour. Specifications regarding the production are provided in Table 1. Water jet machining was used to create test specimens from manufactured laminates following ASTM standards.

## 2.3 Mechanical Properties Testing

### *2.3.1 Hardness measurement*

The shore-D hardness tests were used to determine the composite's hardness. Using a Shore D hardness tester (an HP-E II series; Digital Durometer) under ASTM D2240 regulation [32], the hardness of the composite samples was determined. The fundamental test was evaluating the hardness (depth of the indentation) and applying the force consistently and shock-free. To obtain the aggregate findings, each sample on the composite must have at least 10 indentation points.

### *2.3.2 Interlaminar shear test*

Three-point bending test was performed to evaluate the ILSS of the nanocomposite samples following ASTM D2344 [33]. Short beams of 24 mm × 6.25 mm × 3 mm were tested at a cross-head speed of 0.75 mm/min, amid five samples per configuration. The mean values and standard deviations are given. Equation (1) was utilized to calculate the ILSS:

$$ILSS = \frac{0.75\ P}{b \times t}\ (MPa) \quad (1)$$

### *2.3.3 Flexural test*

Using a three-point bend test at the Universal Testing Machine (UTM Make: Kalpak Instruments, 100 kN), the flexural properties of each sample were determined as per ASTM D790 standard [34]. This apparatus measures the strength of bars that are subjected to uniaxial tensile force and are supported at both ends. The sample sizes are 90 mm × 12 mm × 3.5 mm. A crosshead speed of 25 mm/min was maintained to conduct all samples testing. At 23°C, the experiments were conducted. The flexural modulus was determined by obtaining the load versus deflection curve. Tests on five specimens confirmed the value's consistency. Data were computed using the software of the UTM.

The flexural strength ($\sigma_b$) was computed with the following equation (2):

$$\sigma_b = \frac{3\,PL}{2\,bt^2}\,(MPa) \quad (2)$$

The bending modulus ($E_b$) was calculated using the equation (3):

$$E_b = \frac{L\,m^3}{4\,bt^3}\,(MPa) \quad (3)$$

where $P$ stands for the maximum load applied, $L$ is the effective span between two wedges, $m$ stands for slope of the initial straight line portion of the load-defection curve, $b$ is the width, and $t$ is the thickness of the samples.

#### *2.3.4 Tensile test*

The flat, dumbbell-shaped sample was used for the tensile test more frequently. The specimens measured 110 mm × 10 mm × 3.5 mm. As per ASTM D638-14 [35], all tests were carried out at 23°C using a Kalpak Instruments, 100 kN capacity Universal testing machine at a crosshead speed of 25 mm $min^{-1}$. To confirm the findings, six samples underwent testing. The tensile modulus was determined from the load vs. displacement curve.

#### *2.3.5 Scanning electron microscopy*

Utilizing a scanning electron microscope (Make: JEOL JSM 840A, Japan), the samples of tensile-fractured surfaces were examined. In order to investigate its Fractography features of the fractured surfaces were examined by SEM after gold sputtering to endow with an electrical conducting coating.

## 3. RESULTS AND DISCUSSION

### 3.1 Hardness of G/E and hybrid G/E nanocomposites

Results for hardness (Shore D) of neat G/E and Hnts filled G/E composite samples (H0 to H4) are shown in Figure 2 exhibit a trend that is comparable to the tensile and flexural properties (Figs. 3 and 4). Hardness value of 29 was reported for the G/E samples, but the hybrid nanocomposite containing 6 wt % Hnts had the highest hardness value of 55. The hardness of the G/E composites increased as a result of an increase in the number of high hardness particles (Hnts) inside due to an increase in Hnts loading.

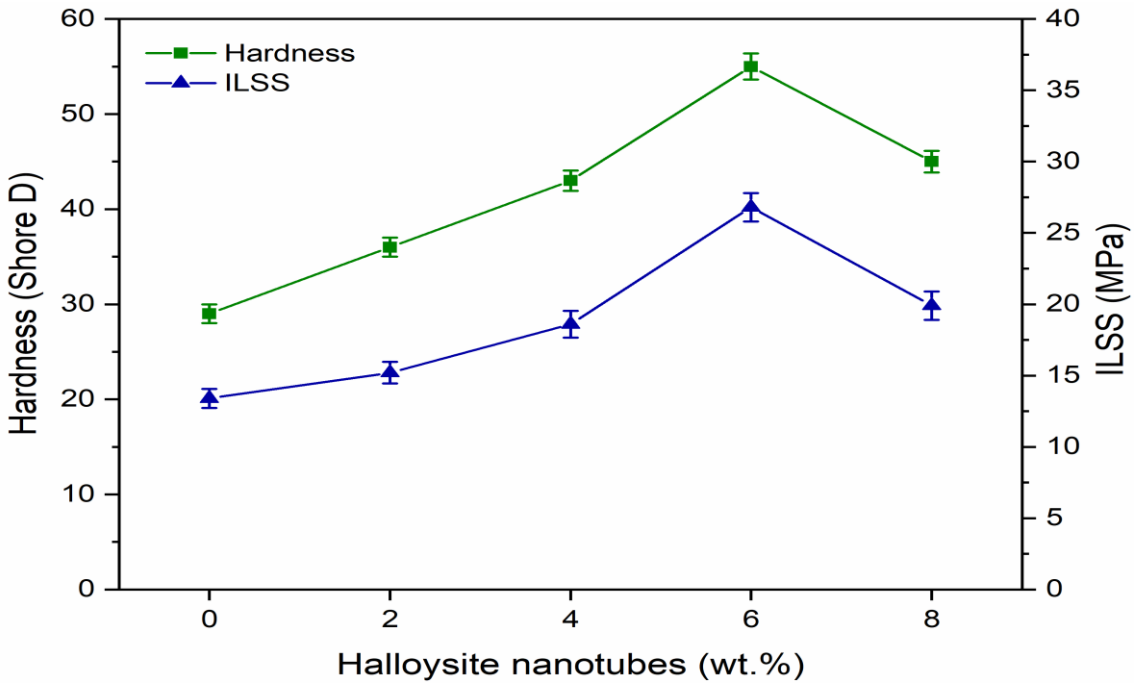


**Fig. 2** Hardness and interlaminar shear strength of G/E and hybrid G/E nanocomposites

### 3.2 Interlaminar shear strength of G/E and hybrid G/E nanocomposites

Interlaminar shear strength (ILSS) of neat G/E and Hnts filled G/E nanocomposites is displayed in Figure 2. In comparison to other nanocomposites and neat G/E composite, the greatest ILSS is determined to be at 6 wt % of the Hnts loaded nanocomposite (H3). ILSS has increased by 100% as a result of the G/E composite containing 6% wt % of Hnts. This may be because of the homogeneous dispersion of Hnts in the epoxy matrix, which strengthened the adhesion between Hnts and the matrix and increased the nanocomposites' shear strength. Nonetheless, samples with an 8 wt % of Hnts loading are observed to have lower ILSS. The less even distribution of Hnts at higher loading might be the cause of this. The SEM pictures of the tensile-fractured surfaces provide proof of this (Fig. 5).

### 3.3 Flexural properties of G/E and hybrid G/E nanocomposites

Flexural strength and modulus are plotted vs wt % of Hnts in the G/E nanocomposites in Figure 3. The findings showed that flexural strength and flexural modulus improved by up to 6 wt % with an increase in the wt % of Hnts. The hybrid nanocomposites containing 6 wt % Hnts showed the greatest enhancement in flexural strength and modulus from 375.9 MPa to 475.6 MPa and 8743.4 MPa to 9814.9 MPa, respectively. However, as the wt % of Hnts greater than 6 wt % in G/E composite, flexural properties decreased. Better interface bonding between glass fiber/Hnts and epoxy matrix is responsible for the increase in flexural strength

and modulus (SEM images in Fig. 5). It might also be because the G/E composites contain high strength and modulus Hnts nanoparticles.

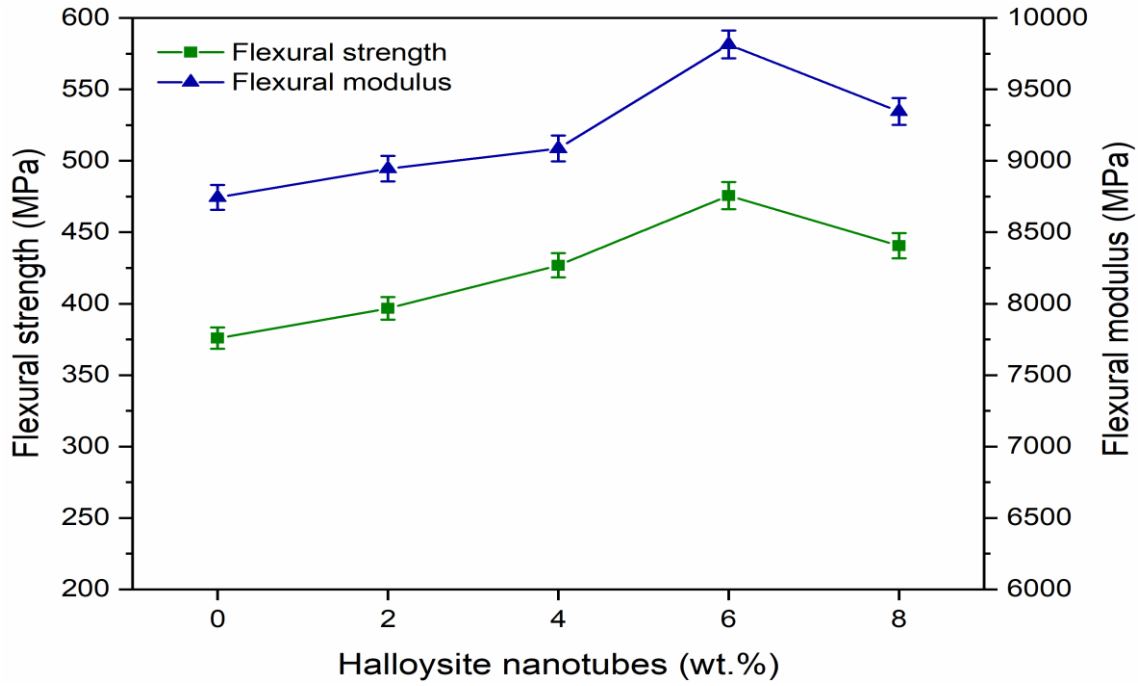


**Fig. 3** Flexural strength and modulus of G/E and hybrid G/E nanocomposites

Moreover, the van der Waals' force among two nanoparticles augmented with an increase in Hnts loading (>6 wt %), which causes the nanoparticles to agglomerate in the G/E composite. At the fiber-matrix interface, the agglomerated nanoparticles' decreased active surface area for interaction with the epoxy matrix leads to inefficient load transfer. The decrease in flexural properties of the 8 wt % Hnts modified hybrid nanocomposites can also be attributed to the void content. In 6 wt % Hnts into G/E composite, the greatest augmentation of flexural strength and flexural modulus were observed to be around 26.5% and 12.3%, respectively.

### 3.4 Tensile properties of G/E and hybrid G/E nanocomposites

The tensile strength and tensile modulus of the neat G/E and Hnts filled G/E hybrid nanocomposites under tensile load are depicted in Figure 4. The G/E with 6 wt % of Hnts (H3) sample, displaying peak values for tensile strength and modulus. When compared to H0, the tensile strength and modulus of the H1 nanocomposite were enhanced by 2.3% and 5.6%, respectively. According to Alhuthali and Low [36], the addition of Hnts enhanced the elastic

modulus of recycled cellulose fiber/vinyl ester near 162.3%. Nonetheless, the presence of voids in the nanocomposites may have contributed to the decreased strength. One of the likely ways to minimize voids and enhance the interface and interphase strength of F-RPCs is to incorporate nanofiller [37]. To improve the required properties, the nanofillers are essentially mechanically entangled or chemically bound with the polymer matrix [38].

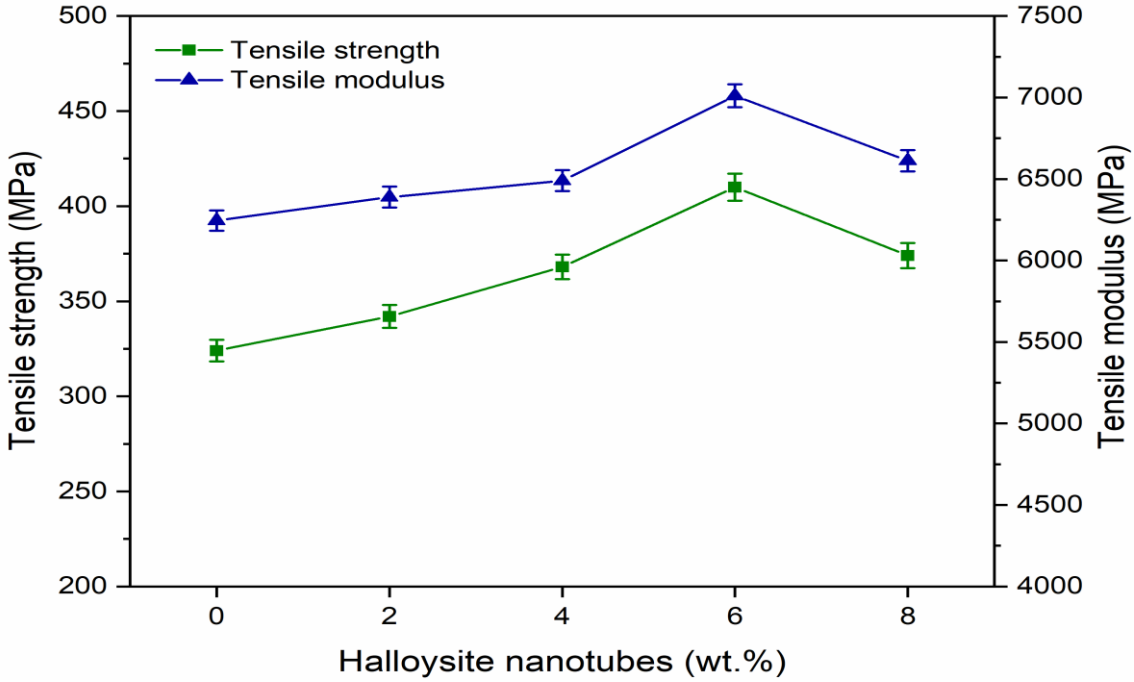


**Fig. 4** Tensile strength and modulus of G/E and hybrid G/E nanocomposites

This research work showed that an increase in Hnts up to 6 wt % was associated with a common behaviour of an increase in tensile strength and modulus for G/E composite. In comparison to H0, the modulus and tensile strength of the 6% wt % Hnts filled G/E (H3) rose by 12.3% and 26.5%, respectively. This enhancement in tensile strength and modulus is due to the nanoparticles' excellent dispersion and interfacial adhesion. Tensile strength and modulus showed a small decline in the 8 wt % Hnts filled G/E composites (H4). The tensile strength and modulus of G/E composite samples with a greater weight percentage (>6 wt %) of nanoparticles decreased due to the existence of an agglomeration. Instead of transferring load, this concentrates stress, and failure ensues.

The enhancement or declining of mechanical properties could be associated with the structure of the fracture surface to prop up the new findings. Figure 5 shows the SEM photomicrographs of the fractured zone of neat G/E, 6 wt % and 8 wt % Hnts filled G/E composites under tensile load. Figure 5(a), (b), and (c) shows the tensile fractured SEM

images of Ho, H3 and H4 composite samples respectively. The fractured was observed to be brittle.

The fractured surface of neat G/E composite is as shown in Figure 5(a). From Figure 5(a) the fracture is almost at right angles to the fiber axis. Clean and smooth fiber-pull out holes are seen from the fractured surface. It is because of weakening of the interface bond between matrix and fiber. The broken fibers perceptible are long and failure of epoxy matrix occurred first and fibers are visible to take the load further. Apart from the high load, we have seen improper bonding between fibers and epoxy matrix. Because of the superficial fiber and matrix connection, an effective load transfer was seen from matrix to fiber.

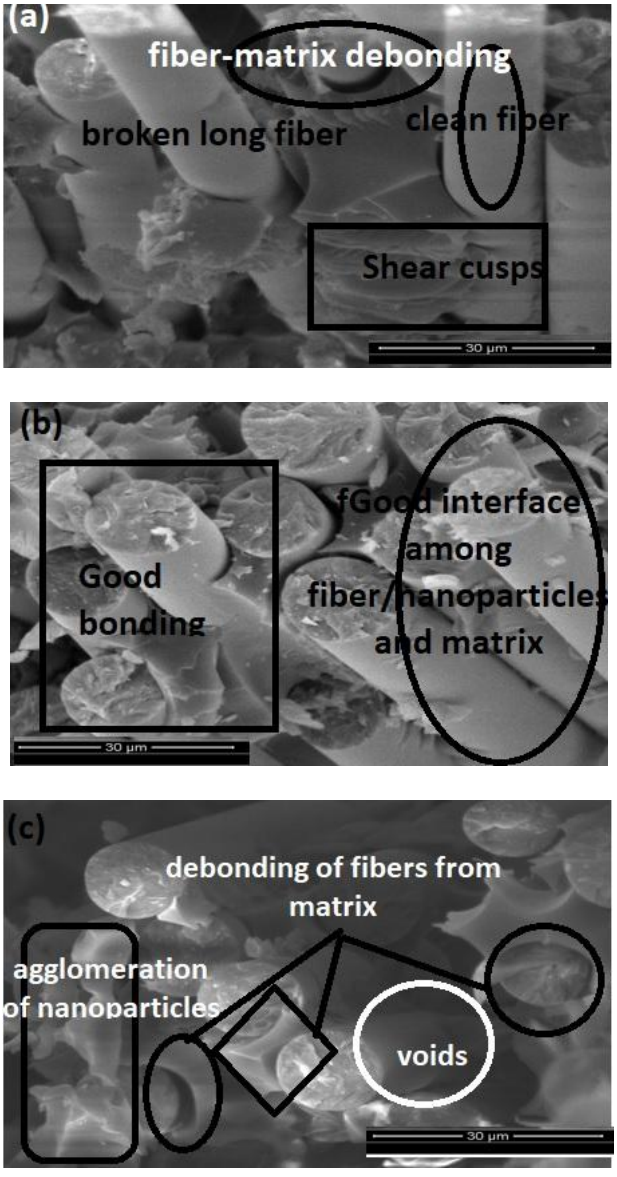


**Fig. 5** SEM micrographs of fracture surface of (a) Neat G/E, (b) H3 (6 wt % Hnts), (c) H4 (8 wt % Hnts)

Figure 5(b) shows the photomicrograph of H3 composite sample. Figure 5(b) shows the toughen matrix and shear cusps in the matrix, which implies the enrichment of mechanical characteristics of hybrid nanocomposites. This figure clearly indicates that Hnts were beneficial in enhancing the interface between fiber and matrix away from a certain loading. Furthermore, SEM micrograph shows strengthening mechanism of 6 wt % of Hnts in G/E composite. Therefore, it can be said that the mechanical characteristics of H3 composite samples are improved by the toughened matrix and good interface bond. We can see that the fiber failure is at an angle to the fiber axis in Figure 5(c). This figure illustrates how the agglomeration of Hnts contributes to a decrease in the mechanical characteristics of G/E nanocomposites containing 8% Hnts.

## 4. CONCLUSIONS

Evaluation and reporting of the impact of Hnts loading on the mechanical characteristics of neat G/E composite and its hybrid nanocomposites were done. The following are the conclusions.

I. The G/E composite's hardness and interlaminar shear strength rose when Hnts loading reached 6 wt % and declined as Hnts loading continued. When compared to other hybrid nanocomposites and neat G/E composite, the interlaminar shear strength of the nanocomposite containing 6 wt % of Hnts enhanced by 100%. The consistent dispersion of Hnts in epoxy, as shown by SEM, improved the interface between the nanoparticles and the matrix, leading to notable improvements in hardness and interlaminar shear strength observed in 6 wt % Hnts nanocomposites.

II. At first, the flexural modulus and flexural strength rises as the G/E nanocomposites' Hnts loading increases. With 6% wt % of Hnts, the hybrid nanocomposites flexural strength increased by 26.5%. It results from improved interface bonding between the matrix and fiber as well as matrix toughening. Additionally, in G/E composite, the flexural modulus rises as the Hnts loading increases up to 6% weight percentage. Nevertheless, if Hnts loading increases further, a negative impact has been noted because to nanoparticles agglomeration.

III. In comparison to H0, the modulus and tensile strength of the 6% wt % Hnts filled G/E (H3) rose by 12.3% and 26.5%, respectively. This enhancement in tensile strength and modulus is due to the nanoparticles' excellent dispersion and interfacial adhesion.

However, the tensile strength and modulus of G/E composite samples with a greater weight percentage (>6 wt %) of Hnts decreased due to the existence of an agglomeration.

IV. Toughen matrix and shear cusps in the matrix, which implies the enhancement of mechanical properties of G/E nanocomposites. The fracture morphologies of clearly indicates that the Hnts were beneficial in improving the interface between the fiber and matrix material beyond a certain loading.

## ACKNOWLEDGMENTS

Authors express a gratitude for the principal, NIE Mysore and Head of the department (Mechanical Engineering) NIE Mysore for providing the opportunity to work and conduct experiments. Authors also thank Head of the department, PST, JSS S & T University for providing the SEM facility. Finally, authors also remember the efforts of Mr. Byresh for extending the hands in carrying out the experimentations.

## AUTHORS CONTRIBUTION

The manuscript was written with the assistance of all contributors. All authors have given their full permission for the final paper.

## DECLARATION OF COMPETING INTEREST

The authors declare that they have no known competing financial interests or personal relationships that could have appeared to influence the work reported in this paper.

## REFERENCES

1. Fałtynowicz, H., Kułażynski, M. and Goodman, S.H., 2022. Epoxies. In *Handbook of Thermoset Plastics* (pp. 175-229). William Andrew Publishing.
2. Jin, F.L., Li, X. and Park, S.J., 2015. Synthesis and application of epoxy resins: A review. Journal of industrial and engineering chemistry, 29, pp.1-11.
3. de Luzuriaga, A.R., Rekondo, A., Martín, R., Markaide, N., Odriozola, I. and Cabañero, G., 2016. Reworkable, recyclable and repairable thermoset epoxy composites in transportation applications. In FORM Forum (Vol. 196, pp. 1-9).
4. Agarwal, S. and Gupta, R.K., 2018. The use of thermosets in the building and construction industry. In Thermosets (pp. 279-302). Elsevier.
5. Suresha, B., Chandramohan, G., Renukappa, N.M. and Siddaramaiah, 2007. Mechanical and tribological properties of glass–epoxy composites with and without graphite particulate filler. Journal of applied polymer science, 103(4), pp.2472-2480.

6. Suresha, B., Chandramohan, G., Kishore, Sampathkumaran, P. and Seetharamu, S., 2008. Mechanical and three-body abrasive wear behaviour of SiC filled glass-epoxy composites. Polymer Composites, 29(9), pp.1020-1025.
7. Suresha, B., Chandramohan, G., Renukappa, N.M. and Siddaramaiah, 2009. Influence of silicon carbide filler on mechanical and dielectric properties of glass fabric reinforced epoxy composites. Journal of applied polymer science, 111(2), pp.685-691.
8. Manjunath, M., Renukappa, N.M. and Suresha, B., 2016. Influence of micro and nanofillers on mechanical properties of pultruded unidirectional glass fiber reinforced epoxy composite systems. Journal of Composite Materials, 50(8), pp.1109-1121.
9. Suresha, B., Vidyashree, S. and Bettegowda, H., 2023. Effect of Filler Materials on Abrasive Wear Performance of Glass/Epoxy Composites. Tribology in Industry, 44(1), p.111.
10. Kuruvilla, S.P., Renukappa, N.M. and Suresha, B., 2020. Dynamic mechanical properties of glass fiber reinforced epoxy composites with micro and nanofillers. In Techno-Societal 2018: Proceedings of the 2nd International Conference on Advanced Technologies for Societal Applications-Volume 2 (pp. 337-347). Springer International Publishing.
11. Suresha, B., Varun, C.A., Indushekhara, N.M. and Vishwanath, H.R., 2019, July. Effect of nano filler reinforcement on mechanical properties of epoxy composites. In IOP conference series: Materials science and engineering (Vol. 574, No. 1, p. 012010). IOP Publishing.
12. Suresha, B., Rajamurugan, G. and Megalingam, A., 2018. Mechanical and abrasive wear behavior of cenosphere filled carbon reinforced epoxy composites using Taguchi-Grey relational analysis. Materials Research Express, 6(1), p.015307.
13. Khammassi, S., Tarfaoui, M. and Lafdi, K., 2021. Study of mechanical performance of polymer nanocomposites reinforced with exfoliated graphite of different mesh sizes using micro-indentation. Journal of Composite Materials, 55(19), pp.2617-2629.
14. Sasidharan, S. and Anand, A., 2020. Epoxy-based hybrid structural composites with nanofillers: a review. Industrial & Engineering Chemistry Research, 59(28), pp.12617-12631.
15. Kostagiannakopoulou, C., Tsilimigkra, X., Sotiriadis, G. and Kostopoulos, V., 2017. Synergy effect of carbon nano-fillers on the fracture toughness of structural composites. Composites Part B: Engineering, 129, pp.18-25.
16. Rajhi, A.A., 2022. Mechanical characterization of hybrid nano-filled glass/epoxy composites. Polymers, 14(22), p.4852.
17. Lal, A.; Markad, K. Thermo-mechanical post buckling analysis of multiwall carbon nanotube-reinforced composite laminated beam under elastic foundation. Curved Layer. Struct. 2019, 6, 212–228.
18. Mostovoy, A. Fiber-Reinforced Polymer Composites: Manufacturing and Performance. Polymers 2022, 14, 338.
19. Jamali, N.; Rezvani, A.; Khosravi, H.; Tohidlou, E. On the mechanical behavior of basalt fiber/epoxy composites filled with silanized graphene oxide nanoplatelets. Polym. Compos. 2018, 39, E2472–E2482.
20. Chang, M.S. An investigation on the dynamic behavior and thermal properties of MWCNTs/FRP laminate composites. J. Reinf. Plast. Compos. 2010, 29, 3593–3599.
21. Vázquez-Moreno, J.M.; Sánchez-Hidalgo, R.; Sanz-Horcajo, E.; Viña, J.; Verdejo, R.; López-Manchado, M.A. Preparation and Mechanical Properties of Graphene/Carbon Fiber-Reinforced Hierarchical Polymer Composites. J. Compos. Sci. 2019, 3, 30.
22. Veena, M.G., Renukappa, N.M., Suresha, B. and Shivakumar, K.N., 2011. Tribological and electrical properties of silica-filled epoxy nanocomposites. Polymer Composites, 32(12), pp.2038-2050.
23. Tian, Y.; Zhang, H.; Zhang, Z. Influence of nanoparticles on the interfacial properties of fiber-reinforced-epoxy composites. Compos. Part A Appl. Sci. Manuf. 2017, 98, 1–8.
24. Zheng, Y.; Ning, R.; Zheng, Y. Study of Si02 nanoparticies on the improved performance of epoxy and fibre composites. J. Reinf. Plast. Compos. 2005, 24, 223–233.
25. Levis, S.R. and Deasy, P.B., 2002. Characterisation of halloysite for use as a microtubular drug delivery system. International Journal of Pharmaceutics, 243(1-2), pp.125-134.

26. Abdullayev, E., Lvov, Y., 2013. Halloysite clay nanotubes as a ceramic ‘‘skeleton” for functional biopolymer composites with sustained drug release. J. Mater. Chem. B 1 (23), 2894–2903.
27. Kushwaha, S.K.S., Kushwaha, N., Pandey, P., Fatma, B., 2021. Halloysite Nanotubes for Nanomedicine: Prospects, Challenges and Applications. BioNanoScience 11 (1), 200–208.
28. Wu, Y., Zhang, Y., Ju, J., Yan, H., Huang, X., Tan, Y., 2019. Advances in Halloysite Nanotubes-Polysaccharide Nanocomposite Preparation and Applications. Polymers 11 (6), 987
29. El-baky, M.A.A. and Attia, M.A., 2022. The mechanical performance of the laminated aluminum-epoxy/glass fiber composites containing halloysite nanotubes: An experimental investigation. Journal of Industrial Textiles, 51(5_suppl), pp.8690S-8737
30. S.Lapčík, L., Sepetcioğlu, H., Murtaja, Y., Lapčíková, B., Vašina, M., Ovsík, M., Staněk, M. and Gautam, S., 2023. Study of mechanical properties of epoxy/graphene and epoxy/halloysite nanocomposites. Nanotechnology Reviews, 12(1), p.20220520.
31. Romanov, V.S., Lomov, S.V., Verpoest, I. and Gorbatikh, L., 2015. Stress magnification due to carbon nanotube agglomeration in composites. Composite Structures, 133, pp.246-256.
32. ASTM D2240-15(2021)-Standard Test Method for Rubber Property—Durometer Hardness, (West Conshohoken, PA, USA: ASTM International).
33. ASTM D2344/D2344M-22 -Standard Test Method for Short-Beam Strength of Polymer Matrix Composite Materials and Their Laminates
34. ASTM D790-17-Standard Test Methods for Flexural Properties of Unreinforced and Reinforced Plastics and Electrical Insulating Materials.
35. ASTM D638-14, Standard Test Method for Tensile Properties of Plastics Trans (ASTM International).
36. Alhuthali, A.M. and Low, I.M., 2013. Influence of halloysite nanotubes on physical and mechanical properties of cellulose fibres reinforced vinyl ester composites. Journal of Reinforced Plastics and Composites, 32(4), pp.233-247.
37. X.J. Fan, S.W.R. Lee, Q. Han, 2009. Experimental investigations and model study of moisture behaviors in polymeric materials, Microelectron. Reliab. 49, pp. 861–871.
38. Y. Hu, G. Du, N. Chen, 2016. A novel approach for $Al_2O_3$/epoxy composites with high strength and thermal conductivity, Compos. Sci. Technol. 124, pp.36–43.